Validation of MODIS aerosol optical depth retrievals over a tropical urban site, Pune, India

Sanjay More[1], P. Pradeep Kumar[1], Pawan Gupta[2][3], P. C. S. Devara[4], G. R. Aher[5]*
[1] Department of Atmospheric and Space Sciences, University of Pune – 07
[2] NASA Goddard Space Flight Center Greenbelt, MD 20771, USA
[3] Universities Space Research Association, Greenbelt, MD 20771, USA
[4] Indian Institute of Tropical Meteorology, Pune-08
[5] Physics Department Nowrosjee Wadia College, Pune-01
aher.g.r@gmail.com

Summary

This paper attempts to validate the MODIS dark target aerosol optical depth product over tropical urban location in India. The ground truth data used in this study has been collected using Microtops hand held sun-photometer on cloud free days during 2008-2010. AERONET measurements have also been compared against MODIS and Microtops. Aerosol properties derived from the AERONET over the same location have been analyzed as well. This is the first ever systematic validation of the MODIS aerosol products over Pune. MODIS AOD retrievals are well correlated with the AERONET and Microtops AODs. MODIS AODs underestimate during winter and overestimate during pre-monsoon. MODIS retrievals are capable of characterizing AOD distributions over Pune. Systematic error in the MODIS aerosol products needs further investigation. Single scattering albedo shows seasonal variability, winter months were dominated by absorbing type of aerosols whereas summer time scattering aerosols dominates the AOD values. Both winter and pre monsoon months do not shows large diurnal variations at the station.

Validation of MODIS aerosol optical depth retrievals over a tropical urban site, Pune, India

Sanjay More[1], P. Pradeep Kumar[1], Pawan Gupta[2,3], P. C. S. Devara[4], G. R. Aher[5*]

[1] Department of Atmospheric and Space Sciences, University of Pune – 07
[2] NASA Goddard Space Flight Center Greenbelt, MD 20771, USA
[3] Universities Space Research Association, Greenbelt, MD 20771, USA
[4] Indian Institute of Tropical Meteorology, Pune-08
[5] Physics Department Nowrosjee Wadia College, Pune-01
*aher.g.r@gmail.com

Abstract

In the present paper, MODIS (Terra and Aqua; level 2, collection 5) derived aerosoloptical depths (AODs) are compared with the ground-based measurements obtained from AERONET (level 2.0) and Microtops - II sun-photometer over a tropical urban station, Pune ($18°32'$N; $73°49'$E, 559 m amsl). This is the first ever systematic validation of the MODIS aerosol products over Pune. Analysis of the data indicates that the Terra and Aqua MODIS AOD retrievals at 550 nm have good correlations with the AERONET and Microtops - II sun-photometer AOD measurements.

During winter the linear regression correlation coefficients for MODIS products against AERONET measurements are 0.79 for Terra and 0.62 for Aqua; however for pre-monsoon, the corresponding coefficients are 0.78 and 0.74. Similarly, the linear regression correlation coefficients for Microtops measurements against MODIS products are 0.72 and 0.93 for Terra and Aqua data respectively during winter and are 0.78 and 0.75 during pre-monsoon. On yearly basis in 2008-2009, correlation coefficients for MODIS products against AERONET measurements are 0.80 and 0.78 for Terra and Aqua respectively while the corresponding coefficients are 0.70 and 0.73 during 2009-2010. The regressed intercepts with MODIS vs. AERONET are 0.09 for Terra and 0.05 for Aqua during winter whereas their values are 0.04 and 0.07 during pre-monsoon. However, MODIS AODs are found to underestimate during winter and overestimate during pre-monsoon with respect to AERONET and Microtops measurements having slopes 0.63 (Terra) and 0.74 (Aqua) during winter and 0.97 (Terra) and 0.94 (Aqua) during pre-monsoon.

Wavelength dependency of Single Scattering Albedo (SSA) shows presence of absorbing and scattering aerosol particles. For winter, SSA decreases with wavelength with the values 0.86 ±0.03 at 440 nm and 0.82 ±0.04 at 1020nm. In pre-monsoon, it increases with wavelength (SSA is 0.87 ±0.02 at 440nm; and 0.88 ±0.04 at 1020 nm).

1. Introduction

The knowledge of spatial and temporal distributions of aerosols on regional and global scale is essential to understand the dynamics of aerosols and the associated influence on regional and global climatic conditions (Tripathi et al., 2005). Satellites-based remote sensing technique provides systematic retrieval of aerosol optical properties on regional and global scale (Kaufman et al., 2005, Kahn et al., 2010). The MODerate Resolution Imaging Spectroradiameters (MODIS) aboard the Terra (launched in 1999) and Aqua (in 2002) observe the earth-atmosphere systems twice daily. Columnar aerosol optical properties such as aerosol optical depth (AOD) and aerosol small mode fraction (ASMF) are retrieved from these observations over both land and ocean (Kaufman et al., 1997; Tanre et al., 1997). Satellite observations have advantages that they can provide information in the larger spatio-temporal domain (Kaufman et al., 2002) as most of the ground measurements are limited to very small area (point observations). However, aerosols from the space is challenging in areas where surface reflectance is high as it may introduce considerable errors in the derived results. So as to improve the accuracy of the MODIS data, it is essential to compare and validate the MODIS data with independent ground-based measurements. Several research studies have compared and validated MODIS data with the data obtained from the ground-based Microtops II sun – photometers and that measured from federated network instruments viz., Aerosol Robotic Network (AERONET) (Jing-Mei et al., 2010; Retalis et al., 2010; Aloysus et al., 2009; Misra et al., 2008; Levy at al., 2010,Remer et al., 2005; Tripathi et al., 2005; Ichoku et al., 2002a; Chu et al., 2002; Holben et al., 1998, Hyer et al., 2011). Since the

2

23   launch of MODIS, validation studies suggested that the expected error (EE) over land

24   could be represented by EE = ± 0.05 ±0.15xAOD (Remer et al., 2005).

25   In India, several validation of MODIS derived AOD has been carried out by

26   various groups (Jethva et al., 2005, Tripathi et al., Prasad and Singh, 2007). Tripathi et

27   al., (2005) using MODIS level 2 and collection 4 AOD data with AERONET data for

28   2004 found an overestimation by MODIS during dust and an underestimation during non-

29   dust seasons having slopes and intercepts in the two cases 2.46, -0.63 and 0.69, 0.12

30   respectively with nearly same correlation coefficients (0.72 and 0.71 respectively). For

31   the Indo-Gangatic basin, Jethva et al.,(2005) compared the monthly mean AOD at 550

32   nm from MODIS level 3 daily gridded data with AERONET sunphotometer derived

33   monthly mean AOD values for Kanpur, India during January 2001 to July 2003 and

34   found a systematic overestimation by MODIS during summer and underestimation

35   during winter. Prasad and Singh (2007) also found MODIS overestimating AOD values

36   during summer and underestimating during winter with the slopes and intercepts with two

37   cases 0.51, 0.52 and 0.48, 0.15 respectively. The correlation coefficients in the two cases

38   were less than 0.5.

39   In the present study, we compare MODIS (Terra and Aqua) AOD retrievals with

40   AERONET AODs of level 2.0 and Microtops II sun-photometer measurements at Pune

41   (18°32'N; 73°49'E, 559 m amsl), India. CIMEL sun-sky radiometer installed at Indian

42   Institute of Tropical Meteorology (IITM) as a part of AERONET global network, and it

43   makes measurements at 440, 675, 870, 940, and 1020nm and three polarized channels at

44   870 nm. In the present study, data retrieved from 440, 675, 870 and 1020 channels are

45   used The Microtops II sun-photometer (five channels) is operated from Pune University

3

46   campus on cloud free days observing seasons spanning over Dec-May for the period

47   2008-09 and 2009-10. To the best of our knowledge this is the first kind of systematic

48   study that validates MODIS data over Pune. The study also presents seasonal behaviour

49   of AERONET inversion products viz., aerosol columnar volume size distribution

50   (ACVSD), single scattering albedo (SSA), and Angstrom Exponent (α).

51   **2. Study Location and Local Meteorology:**

52   The study location, over which the validation has been performed, is Pune ($18^0 32^{'}$ N;

53      $73^0 49^{'}$ E, 559m amsl). It is about 100 km from the west cost of India and Lee-ward side of

54   Sahyadri Range (Western Ghats). Pune has tropical wet and dry climate. Figure (1)

55   shows the NCEP /NCAR reanalysis mean vector wind composites at 850 hPa for winter

56   and pre-monsoon seasons during 2009 and 2010 over the Indian region (0 – 40^0 N; 60 –

57   100^0 E). In winter (Dec, Jan and Feb), minimum temperature is up to 3 to 4^0C with light

58   winds and continental air mass passing over the region. During the Pre-monsoon (Mar,

59   Apr and May) the weather is very hot with the maximum temperature of about 40^0 C and

60   surface winds mostly gusty and dust content in the atmosphere is maximum.

61   The study region mainly comprises of semi arid region and has six types of land

62   use and land cover as shown in Figure (2). It mainly consist of fallow land (39.42%),

63   dense scrub (20.88%), agriculture land (15.96%), settlement (13.02%), vegetation

64   (9.51%) and water body (1.18%). It contains 377 villages and has a population of 44,

65   54,509 (Census of India 2001). The population and the number of vehicles and

66   industrialization has been increasing at a steady rate over pune since 2001.

67

68 **3. Data and Methodology:**

69 **3.1 Data**

70 MODIS data are available at different processing levels, level 1.0 (geolocated &

71 calibrated brightness temperatures and radiances), level 2.0 (derived geophysical data

72 products) and level 3.0 (Gridded time-averaged product) (King et al., 2003). AERONET

73 data are also available at three different levels, level 1.0 (raw or unscreened data), level

74 1.5 (cloud screened data) and level 2.0 (quality assured data) (Holben et al., 1998). For

75 this study, we have employed MODIS (both Terra & Aqua) level 2 collection 5

76 instanteneous AOD data at 550 nm.. MODIS AOD retrievals are compared with level 2.0

77 AERONET and Microtops II sun-photometer measurements of AODs.

78 **3.2 MODIS**

79 Radiant energy reflected and emitted by the Earth carries a signature of atmospheric and

80 surface properties. Satellite sensors can quantify several atmospheric properties by

81 measuring the wavelength, angular and polarization properties of this radiant energy

82 (Kaufman et al., 2002). The MODIS has been designed with aerosol and cloud remote

83 sensing in mind (King et al., 1992). It is sun-synchronous and near polar orbiting, with a

84 circular orbit of 705 km above the surface. MODIS has 36 bands ranging from 0.4 to 14.4

85 μm wavelengths with three different spatial resolutions (250, 500 and 1000 m) and views

86 the Earth with a swath of 2330 km thereby observing the entire globe every day, with

87 equatorial crossing local time 10:30 am and 1:30 pm (Terra and Aqua respectively).

88   The MODIS retrievals of aerosol use two separate algorithms for land and ocean.

89 Both the algorithms were developed before the Terra launch and are well described in

90 Kaufman et al. (1997) for land and Tanre et al. (1997) for ocean. MODIS retrievals of

91 AOD over land uses three spectral channels centered at 0.47, 0.66, and 2.13 μm

92 wavelength. The retrieval of AOD is performed and reported at 10x10 km^2 pixel size

93 although the original observations are made at 250-1000m resolution. Each high

94 resolution pixel in the 10x10km^2 box is evaluated for cloud, ice/snow and then mean

95 reflectance values are utilized to retrieve AOD using lookup table approach. More details

96 on AOD retrieval can be found elsewhere [i.e. Remer et al., 2005, Levy et al., 2007a,

97 2007b]

3.4 AERONET (AErosol RObotic NETwork)

99 The AERONET (AErosol RObotic NETwork) is a federation of ground-based

100 remote sensing aerosol networks established by NASA and is greatly expanded by

101 collaborators from other agencies. The program provides a long-term, continuous

102 database of aerosol optical, microphysical and radiative properties for aerosol research

103 and characterization, validation of satellite retrievals, and synergism with other databases.

104 The network imposes standardization of instruments, calibration, processing and

105 distribution.

106 AERONET provides globally distributed observations of spectral AOD, inversion

107 products, and precipitable water in various aerosol regimes. It employs CIMEL sun-sky

108 spectral radiometer which measures the direct sun radiances at eight spectral channels

109 centered at 340, 380, 440, 500, 670, 870, 940 and 1020 nm. The accuracy of direct sun

110 measurements are within ±0.01 and ±0.02 for larger wavelengths (greater than 440 nm)

111 and shorter wavelength (Holben et al., 1998; Eck et al., 1999). Optical depth is calculated

112 from spectral extinction of direct beam radiation at each wavelength based on the

6

113 Lambert-Beer-Bouguer Law. Aerosol optical depth (AOD) is determined by correcting

114 optical depth for attenuation due to Rayleigh scattering, absorption by ozone and gaseous

115 pollutants. In addition to direct solar radiance, instrument also measures the diffuse sky

116 radiance at four spectral bands (440, 670, 870 and 1020 nm) along the solar principal

117 plane and solar almucantar through a constant aerosol profile to retrieve size distribution,

118 phase function and AOD (Holben et al., 1998).

119 Indian Institute of Tropical Meteorology (IITM) is one of the stations of this

120 network. CIMEL sun/sky radiometer is installed in the campus of IITM and continuously

121 operational since 2004 (Sumit and Devara, 2011). The automatic sun-sky tracking

122 radiometer at IITM makes measurements with a 1.2^0 full field of view at every ~15 min

123 interval at five spectral channels (440, 675, 870, 940, 1020nm). In this study data

124 retrieved form 440, 675, 870 and 1020 nm are used for its comparison with MODIS AOD

125 retrievals. To determine aerosol columnar volume size distribution and Single Scattering

126 Albedo (ω_o) solar principal plane (constant azimuth angle, with varied scattering angles)

127 and solar almucantar (constant elevation angle, with varied azimuth angles) geometry is

128 used at 440, 675, 870 and 1020 nm.

129 **3.5 Microtops II Sun-photometer**

130 The ground based measurements have been carried out at Pune University campus

131 ($18^032^{'}$N; $73^049^{'}$E) using handheld Microtops II Sun-photometer from morning till

132 evening at an interval of 10 min. during 2008-09 and 2009-10 on clear sky days. The

133 instrument is well calibrated (Manufactured by Solar Light Company, Philadelphia,

134 USA.). The design, calibration and performance details have been described by Devara et

135 al., (2001) and Morys et al., (2001). The expected accuracy of the sun-photometer

136 retrievals is comparable with those of CIMEL sun-photometer used in AERONET

137 network with uncertainties in the range of 0.01 to 0.02 (Ichoku et al., 2002b). The

138 instrument measures the intensity of direct solar irradiance at five spectral narrow band

139 spectral channels centered at 440, 500, 675, 870 and 1020 nm. From this data, AOD

140 value for each wavelength is estimated. These data are used along with AERONET as a

141 "ground truth" for the validation of the MODIS AOD products for this study.

142 **3.6 Methodology**

143 For validation purpose, MODIS retrievals must be collocate in space and time with

144 AERONET and Microtops measurements. We averaged the quality controlled MODIS

145 AOD values at 10 km^2 spatial resolution over 50 km × 50 km grid box centered at ground

146 measurements site. For this, we choose 50 km × 50 km grid box because in larger

147 window size, topography and aerosol type heterogeneity play a role and could bring in

148 errors where as smaller grid box contain insufficient data (Ichoku et al., 2002a).

149 In order to accomplish realistic comparison of AOD's from these instruments viz.,

150 MODIS, AERONET and Microtops II sun-photometer. AERONET and Microtops

151 measured AODs are adjusted to the MODIS derived 550 nm wavelength AODs using the

152 Angstrom exponent (α) and Angstrom turbidity coefficient (β) derived from Microtops

153 and AERONET measured AODs at the wavelengths 440, 500, 675, 870 and 1020 nm

154 (440, 675, 870 and 1020 nm for AERONET) on the corresponding day through a

155 logarithmic regression using the Angstrom empirical formula viz., $AOD = \beta \times \lambda^{-\alpha}$. This

156 yields the corresponding retrieved AOD value at 550 nm for the AERONET and

157 Microtops within ±30 min of MODIS overpass time. Thus, over the two years period (i.e.

158 2008-09 and 2009-10), we obtained 118 and 119 identical data sets for MODIS (Terra)

8

159 and AERONET (48 and 60 data sets for Microtops) during 2008-09 and 2009-10

160 respectively. Similarly, there were 101 and 96 identical data points for MODIS (Aqua)

161 and AERONET (41 and 50 data points for Microtops) during the same period. Thus

162 MODIS -AERONET and MODIS – Microtops data sets form the subject matter of the

163 present paper.

164 **4 Results and Discussion**

165 **4.2 Aerosol Properties**

166 **4.2.1 AOD Variation and Angstrom Exponent (α)**

167 The spectral variation of aerosol optical depth and frequency distribution of α

168 during winter and pre-monsoon season for the period of Dec 2008-May 2010 over Pune

169 is shown in Figure 3(a b). Seasonal variation of α is monomodal in winter and bimodal

170 in pre-monsoon. The modal value of α of 1.4 during winter suggests dominance of

171 submicron aerosol particles originating from anthropogenic activity like fossile fuel

172 combustion and biofuel burning (Pandithurai et al., 2007, Venkataraman et al., 2005,).

173 During pre-monsoon, bimodal nature of α has modal values 0.5 and 0.95 indicating that

174 dominance of both fine and coarse mode particles. This reveals that the aerosol system

175 over Pune is controlled by different sources.

176 Figure (4) reveals monthly mean value of aerosol optical depth and α obtained from

177 AERONET measurements during Dec2008-May2010. From the figure, high AE values at

178 low AODs during winter and low α at high AOD values during pre-monsoon also

179 indicates the dominance of fine mode and coarse mode particles in winter and pre-

180 monsoon respectively.

9

181   **4.2. 2 Aerosol Columnar Volume Size Distribution**

182   Atmospheric aerosols, which come from many natural and man-made sources,

183   present a wide range of particle sizes and concentrations. Their behavior and the

184   atmospheric effects produced by them depend on their size. The inversion algorithm

185   developed by Dubovik and King (2000) has been used.

186   Results of this analysis are given in Figure (5) which depicts seasonal variation of

187   aerosol columnar volume size distribution over Pune using AERONET data during the

188   period Dec 2008 – May 2010. It is clear from the figure that the modal volume size

189   concentration of both accumulation mode (< 1 μm) and coarse mode (> 1 μm) are low

190   during winter. As compared to winter, during pre-monsoon there is no considerable

191   change in accumulation mode but there is significant increase in modal volume

192   concentration (about 1.5) for the coarse mode. The dominance of coarse mode particles

193   may be due to dust generation by strong winds (wind blown dust) and strong surface

194   heating. Low value of α (0.85) also supports the dominance of coarse mode particles in

195   pre-monsoon. The sources of fine mode particles are fossil fuel combustion and industrial

196   pollutants.

197   The observed Aerosol Columnar Volume Size Distribution (ACVSD) is found to

198   be bimodal and is represented by

199    $$\frac{dV}{d\ln r} = \frac{V_0}{\sigma(2\pi)} \exp\left(-\frac{\ln[r/r_m]^2}{2\sigma^2}\right)$$ (1)

200   where dV/dlnr is volume size distribution, V_0 is columnar volume of particle per cross

201   section of atmosphere, r is radius, r_m is mode radius and σ is standard deviation of the

202   natural logarithm of particle radii.

10

203   The bimodal nature of volume size distribution may be due to different sources of

204   aerosols such as combination of two air masses with different aerosol origin (Hoppel et

205   al., 1985), generation of new fine particles in the air by the process of heterogeneous

206   nucleation or by homogeneous heteromolecular nucleation and growth of larger particles

207   by condensation of gas-phase reaction products (Singh et al., 2004).

208   The ACVSD parameters and α are given in Table I. During winter, the average values of

209   volume concentration of accumulation mode and coarse mode are 0.020 ±0.016 and

210   0.025 ±0.017 respectively and in pre-monsoon, the corresponding average values are

211   0.022 ± 0.015 and 0.047 ± 0.032. For accumulation mode, the model value of volume

212   concentration (peak) is almost same (0.046 and 0.0.044) for winter and pre-monsoon

213   respectively. For coarse mode, values of volume concentration are 0.053 and 0.087 for

214   winter and pre-monsoon respectively.

215   **4.2.3 Single Scattering Albedo**

216   Single scattering albedo (SSA) is a common measure of the relative contribution of

217   absorption to extinction and is a key variable in assessing the climatic effects of aerosols

218   (Jacobson, 2000; Dubovik et al., 2002). Its value is mostly dependent on the composition

219   and size distribution of aerosols. It is studied by using AERONET inversion product

220   (level 2.0) during Dec 2008 to May 2009. For this, the retrieval algorithm of Dubovik and

221   King (2000) is used to obtain SSA from direct sun and sky radiance measurements by

222   AERONET (CIMEL sun photometer).

223   Figure (6) depicts the wavelength dependence of SSA. During winter, SSA decreases

224   with wavelength having a value 0.86 ±0.03 at 440 nm and 0.82 ±0.04 at 1020nm. Lower

225   SSA at longer wavelength shows dominance of absorbing urban aerosol over Pune,

226   which is attributed to the presence of a mixture of aerosols from multiple sources like

227   vehicular pollution, industrial pollutants, biomass burning in the field. However, in pre-

228   monsoon season, the SSA slightly increases with wavelength (SSA is 0.87 ±0.02 at

229   440nm; and 0.89±0.04 at 1020 nm). This suggests the dominance of coarse particles

230   (mostly dust) during pre-monsoon, which may be either due to local activities like

231   urbanization, industrialization and construction activities or windblown dust due to strong

232   surface heating. Similar observations have been reported by Singh et al., (2004) over

233   Kanpur, Smirnov et al., (2002) in the Persian Gulf, Xia et al., (2005) and Cheng et al.,

234   (2006) over Northern China and Lyamani et al. (2006) over Europe and the

235   Mediterranean region. Monthly variation of SSA for the period of 2008-10 and 2009-10

236   is shown in Figure (7). It reveals that during 2008-09 there is a sharp increase in SSA

237   from Dec to May while the increase is moderate during 2009-10. Seasonal variation and

238   spectral dependence of SSA is well reflected in the monthly variation.

239   **4.3 Inter-comparison between MODIS-AERONET-Microtops II Sun-photometer**

240   **4.3.1 MODIS and AERONET**

241   Figure (8) shows seasonal comparison of MODIS AOD retrievals against

242   AERONET derived AODs, during the winter (Dec-Feb, 2008-2010) and pre-monsoon

243   (Mar-May, 2009-2010). From the figure, it is seen that during winter the correlation

244   coefficient of linear regression fit (R) are 0.79 and 0.62 for Terra and Aqua respectively.

245   While during pre-monsoon the corresponding coefficients are 0.78 and 0.74. These

246   correlation coefficients are significant at 0.01 level. The root mean squared error (RMSE)

247   between the ground based AERONET and MODIS AODs lies in the range 0.09 to 0.10

248   for the data under study.

249   Intercepts of linear regression fit are 0.09 for Terra and 0.05 for Aqua during

250   winter whereas during pre-monsoon intercept values are 0.04 and 0.07 for Terra and

251   Aqua respectively. Slopes of the regressed lines, for Terra and Aqua are 0.63 and 0.74

252   respectively during winter and 0.97 and 0.94 (for Terra and Aqua respectively) during

253   pre-monsoon.

254   Results of regression model for MODIS derived AODs against AERONET

255   measurements at 550 nm during 2008-2009 and 2009-2010 are shown in Table II. It is

256   clear from the table that during 2008-2009 and 2009-2010, MODIS retrievals bear a good

257   correlation with AERONET measurements with correlation coefficients 0.80 and 0.78 for

258   (Terra and Aqua respectively) during 2008-2009 while the corresponding coefficients are

259   0.70 and 0.73 during 2009-2010. Intercept of linear regression model during 2008-2009

260   are 0.05 and -0.01 for Terra and Aqua respectively and the corresponding intercept

261   during 2009-2010 is 0.11 for both Terra and Aqua. Slopes of the regressed line are 0.86

262   and 1.05 during 2008-2009 for Terra and Aqua respectively while during 2009-2010, the

263   corresponding slopes are 0.65 and 0.73.

264   **4.3.2 MODIS and Microtops II Sun-photometer**

265   Figure (9) shows scatter plot of MODIS AOD retrievals against Microtops

266   measured AODs, during the winter (Dec-Feb, 2008-2010) and pre-monsoon (Mar-May,

267   2008-2010). MODIS AOD retrievals also show a good correlation with Microtops II sun-

268   photometer measurements. Correlation coefficients during winter are 0.73 and 0.93 while

269   for pre-monsoon values are 0.78 and 0.75, for Terra and Aqua respectively. RMSE

270 between ground based Microtops II sun-photometer and MODIS AODs lie in the range

271 0.06 – 0.10 for winter and pre-monsoon during the study period.

272   Intercepts of the linear regression fit for MODIS and Microtops AODs are 0.03

273 for Terra and 0.04 for Aqua during winter whereas for pre-monsoon, intercept values are

274 0.05 and 0.09 for Terra and Aqua respectively. Slopes of the regressed lines are 0.54 &

275 0.70 during winter and 0.58 & 0.76 during pre-monsoon for Terra and Aqua respectively.

276 **4.3.3 AERONET and Microtops II Sun-photometer**

277 Figure (10) reveals the scatter plot of AERONET against Microtops at 675nm for all

278 collocated data points during 2008-2010. The linear regression analysis between these

279 data points shows that the correlation coefficient is 0.81 while slope and intercept are

280 0.97 and 0.10 respectively. The seasonal inter-comparison between AERONET and

281 Microtops is shown in Figure (11). It is clear form the Figures (10 and 11) that,

282 Microtops AODs are consistently overestimating compared to those of the AERONET

283 AODs during winter and pre-monsoon over the study period with mean bias is about 0.1

284 in AOD.

285 From the Figures 8 and 9 it is clear that, the MODIS retrievals systematically

286 underestimate during winter and overestimate during pre-monsoon over Pune. Similar

287 results have been reported by Jethva et al.,(2005) and Prasad and Singh (2007) over

288 Kanpur. Monthly variation of AOD using MODIS and AERONET measurements shown

289 in Figure (12) also support this result.

290 The linear regression model for MODIS-AERONET (Fig. 8) and MODIS-Microtops II

291 (Fig 9) and Table II show non-zero intercepts. This indicates that the retrieval algorithm

292 is biased at low AOD values which may be associated with a sensor calibration error or

293 an improper assumption about ground surface reflectance (Tripathi et al., 2005; Zhao et

294 al., 2002). Also, large errors in surface reflectance may lead to large intercepts (Tripathi

295 et al., 2005; Chu et al., 2002).

296 The inconsistency between aerosol microphysical and optical properties used in the

297 MODIS retrieval algorithm and that in the ground truth retrievals generated by

298 AERONET and Microtops is signified by the deviation of the slope from unity. Similar

299 observations have been reported by in other studies (i.e. Jing-Mie , 2010; Tripathi et al.,

300 2005; Zhao et al., 2002).

301 The effect of slope and intercept on the correlation of MODIS derived AODs with

302 AERONET and Microtops measurements shown in Figure (8) and Figure (9) is well

303 represented in the average monthly variation of AOD values from MODIS and

304 AERONET during the study period (2008-10) as shown in Figure (12). Error bars in the

305 figure represent standard deviation of AOD in the month which generally ranges between

306 0.05 - 0.2. The number of days used in the analysis is also indicated on bar chart. It is

307 clear from the figure that the variation patterns of both MODIS (Terra and Aqua) and

308 AERONET AOD data are well matched for both the years with MODIS AOD values

309 relatively lower than those of AERONET AOD values in winter i. e. in relatively low

310 dust period. While in dust loading period (pre-monsoon), MODIS AOD values are higher

311 or tend to be higher than the AERONET AODs. Similar observations have been reported

312 by Tripathi et al., (2005).

313 As overpass time of MODIS Terra and Aqua are 10:30 and 1: 30 respectively the

314 monthly variation of AERONET-Microtops-MODIS-Terra data sets corresponds to

315   monthly variation of AOD during morning hours and that of AERONET-Microtop-

316   MODIS-Aqua to monthly variation of AOD during afternoon. This may be regarded as

317   the diurnal asymmetry in AOD data. This has its origin in the meteorological conditions

318   over Pune. Weather conditions in Pune in winter are conducive to the formation of low

319   level capped inversion of $8 - 10^{\circ}$ K per 100 meter in the atmospheric boundary layer

320   (ABL) during February and to some extent also in March. (Vernekar et al., 1993,

321   Pandhurai et al., 2007). High value of AOD in January/February for Terra and Microtop

322   is produced by the processes such as atmospheric moisture precipitating as haze particles

323   on cold mornings in winter, inversion episodes and the influx of aerosol due to

324   atmospheric circulation as discussed in NCEP/NCAR reanalysis mean vector wind

325   composites at 850 hPa for winter and pre-monsoon seasons (Figure 1). April/May

326   maximum in AOD is normal pre-monsoon high. High value of AOD in pre-monsoon is

327   also a global feature attributed to increased aerosol inputs due to surface heating, wind-

328   blown dust and influx of aerosols (Holben et al., 2001)

329   Seasonal frequency distribution for collocated data points of Terra and Aqua of

330   MODIS and AERONET measured values for 2008-09 and 2009-10 presented in Figure

331   (13). It is clear from the figure that, the frequency distribution is maximum at the range

332   AOD < 0.3 and 0.3-0.4 during winter and pre-monsoon respectively. During winter in the

333   range of AOD < 0.3-04 the frequencies of MODIS AODs are higher than those of

334   AERONET AODs while during pre-monsoon reverse of this case can be seen clearly.

335   The frequencies of MODIS AODs during pre-monsoon found lower than those of

336   AERONET AODs at the range of AOD <0.3-0.5. Maximum frequency difference is 5.86

337   % for winter and 7.04 % during pre-monsoon.

16

338   In the range of AOD > 0.5 MODIS AODs are consistently lower than AERONET

339   AODs during winter while in pre-monsoon in the AOD range > 0.6 MODIS AODs are

340   consistently higher than AERONET AODs. The frequency distribution pattern also

341   supports the underestimation of AOD by MODIS during winter and overestimation

342   during pre-monsoon.

343   **5. Summary and Conclusion**

344   The paper presents the comparison of MODIS AODs (Terra and Aqua) retrievals with

345   ground-based measurements made by AERONET and Microtops II sun-photometer for 2

346   years over a tropical urban station, Pune. The main conclusions from the study are:

347   1. Higher value of α during winter is associated with low AODs and an opposite

348   trend is found to prevalent during pre-monsoon. This confirms occurrence of fine

349   and coarse mode particles during these seasons.

350   2. Aerosol volume size distribution is shows a bimodal distribution during both

351   winter and premonsoon seasons. The volume concentration of coarse mode

352   particles in pre-monsoon is 1.5 times higher as compared to that winter. Similarly,

353   volume concentration of fine mode particles is nearly same in both winter and

354   pre-monsoon. Bimodal structure of volume size distributions indicates the

355   presence of a mixture of aerosols from multiple sources during respective seasons

356   in the atmosphere over Pune.

357   3. The SSA observer over Pune is found to be highly wavelength dependent. It

358   decreases with wavelength in winter indicating the dominance of absorbing

359   aerosols mainly arising from vehicular pollution, industrial pollutants and biomass

360 burning. During pre-monsoon an opposite trend is observed showing the presence

361 of coarse mode particles which may be due to construction activity, wind blown

362 dust and strong surface heating.

363   4. The MODIS AOD retrievals are well correlated with the AERONET and

364   Microtops measurements as indicated by the high correlation coefficients. These

365   are found to be 0.79 for Terra and 0.62 for Aqua during winter; 0.78 for Terra and

366   0.74 for Aqua during pre-monsoon against AERONET data. The corresponding

367   values for Microtops measurements are 0.72 for Terra and 0.93 for Aqua during

368   winter; 0.78 for Terra and 0.75 for Aqua during pre-monsoon with small

369   intercepts.

370   5. MODIS AODs underestimate during winter and overestimate during pre-monsoon

371   with respect to the AERONET and Microtops measurements with slopes less than

372   unity (0.63 for Terra and 0.74 for Aqua during winter; 0.97 for Terra and 0.94 for

373   Aqua during pre-monsoon against AERONET and 0.54 for Terra and 0.70 for

374   Aqua during winter; 0.58 for Terra and 0.76 for Aqua during pre-monsoon against

375   Microtops II sun-photometer).

376   6. Average monthly variation of AODs of MODIS and AERONET shows a similar

377   pattern of variation with MODIS AOD values systematically less than those of

378   AERONET during winter and higher during pre-monsoon. High AODs are

379   observed during January/ February and April/May. Jan/ Feb high is mainly due to

380   higher relative humidity during morning hours, light wind and associated low

381   level capped inversions in the morning. Higher AOD values in April/May are

382   associated with increased aerosol inputs due to surface heating, wind-blown dust

383   and influx of aerosols

384   7. Microtops AODs are consistently overestimating than those of AERONET AODs

385   during the study period with mean bias is about 0.1 in AOD.

386   8. Although, there is systematic error in the MODIS products which needs further

387   investigation. In spite of this, results presented in the present paper indicate that

388   the Terra and Aqua MODIS retrievals are capable of characterizing AOD

389   distributions over tropical urban region Pune.

390

396

397

398

399

400

401

402

403

404

406   **References:**

409   Ackerman, T. P., & Toon O. B. (1981). Absorption of visible radiation in atmosphere

410   containing mixtures of absorbing and non-absorbing particles. *Appied Optics,* 20, 3661–

411   3668, doi:10.1364/AO.20.003661.

410

414   Aloysius M., Mohan M., Babu S. S., Parameswaran K., & Moorthy K. K. (2009).

415   Validation of MODIS derived aerosol optical depth and an investigation on aerosol

416   transport over South East Arabian Sea during ARMEX-II. *Annales Geophysicae,* 27,

417   2285-2296.

415

418   Cheng T., Liu Y., Liu D., Xu Y., & Li H. (2006). Aerosol properties and radiative

419   forcing in Hunshan Dake Desert; northern China. *Atmospheric Envronment,* 40, 2169-

420   2179, doi:10.1016/j.atmosenv.2005.11.054.

419

422   Chu D. A., Kaufman Y. J., Ichoku C., Remer L. A., Tanré D., & Holben B. N. (2002).

423   Validation of MODIS aerosol optical depth retrieval over land. *Geophysical Research*

424   *Letters,* 29 (12), 1617-1621 doi: 10.1029/2001GL013205.

423

427   Devara P. C. S., Maheskumar R. S., Raj P. E., Dani K. K., & Sonbawne S. M., (2001).

428   Some features of columnar aerosol optical depth, ozone and precipitable water content

429   observed over land during the INDOEX-IFP 9. *Meterologische Zeitschrift,* 10 (2), 123-

430   130.

428

428   Dubovik O & King M. D. (2000). A flexible inversion algorithm for retrieval of aerosol

429   optical properties form sun and sky radiance. *Journal of Geophysical Research*, 105

430   (D16), 20673-20696.

431

432   Dubovik O., Holben B. N., King M. D., Tanré D., & Slutsker I. (2002). Variability of

433   absorption and optical properties of kaey aerosol types observed in world wide locations.

434   *Journal of Atmospheric Science*, 59, 590-608.

435

436   Eck T., Holben B. N., Reid J., Dubovik O., Smirnov A., O'Neill N., Slutsker I., & Kinne

437   S. (1999). Wavelength dependence of the optical depth of biomass burning, urban, and

438   desert dust aerosols. *Journal of Geophysical Research*, 104, 31333–31349.

439

440   Holben B. N., Eck T. F., Slutsker I., Danré D., Buis J. P., Setzer A., Vermote E., Reagan

441   J. A., Kaufman Y. J., Nakajima T., Lavenu F., Jankowiak I., & Smirnov A. (1998).

442   AERONET-A federated instrument network and data archive for aerosol characterization.

443   *Remote Sensing of Environment*, 66, 1-16.

444

445   Hoppel W. A., Fitzgerald & Larson R. R. (1985). Aerosol size distribution in air mass

446   advecting off the east coast of the United States. *Journal of Geophysical Research*, 90,

447   2365-2379

448

449   Hyer E. J., Reid J. S., & Zhang J. (2011). An over-land aerosol optical depth data set for

450   data assimilation by filtering, correction, and aggregation of MODIS Collection 5 optical

451 depth retrievals. *Atmospheric Measurement Techniques*, 4 (379), 379-408 doi:

452 10.5194/amt-4-379-2011

453

454 Ichoku C., Chu D. A., Mattoo S., Kaufman Y. J, Remer L. A., Tanré D., Slutsker I., &

455 Holben B. N. (2002a). A spatio-temporal approach for global validation and analysis of

456 MODIS aerosol products. *Geophysical Research Letters*, 29 (12), MOD1-1- MOD 1-4,

457 doi: 10/1029/2001GL013206

458

459 Ichoku C., Levy R., Kaufman Y. J., Remer L. A., Li R. R., Martins V. J., Holben B. N.,

460 Abuhassan N., Slutsker I., Eck T. F., & Pietras C. (2002b). Analysis of the performance

461 characteristics of the five-channel Microtops II sun photometer for measuring aerosol

462 optical thickness and precipitable water vapour. *Journal of Geophysical Research*, 107

463 (D13), 4179, doi: 10.1029/2001JD001302.

464

465 Jacobson M. Z. (2000). A physically based treatment of elemental carbon optics:

466 Implications for global direct forcing of aerosols. *Geophysical Research Letters*, 27, 217-

467 220

468

469 Jethva H., Satheesh S. K., & Srinivasan J. (2005). Seasonal variabilities over the Indo-

470 Gangatic basin. *Journal of Geophysical Ressearch*, 110, D21204, doi

471 10.1029/2005JD005938.

472

473   Jing-Mai A., Jin-Auan Q., & Yan-Liang Y. (2010). Validation of aerosol optical depth

474   from Terra and Aqua MODIS retievelas over a tropical coastal site in China. *Atmospheric*

475   *and Oceanic Science Letters,* 3 (1), 36-39.

476

477   <u>Kahn R.A.,</u> Gaitley B. J., Garay M. J., Diner D. J., Eck T., Smirnov A., and Holben B.

478   N. (2010). MISR global aerosol product assessment by comparison with Aerosol Robotic

479   Network. *Journal of Geophysical Research, 115, D23209,* <u>doi:10.1029/2010JD014601</u>

480

481   Kaufman, Y. J., Tanré D., Ramer L. A., Vermote, E. F., A. Chu., & Holben B. N. (1997).

482   Operational remote sensing of tropospheric aerosols over land from EOS moderate

483   resolution imaging spectroradiometer. *Journal of Geophysical Research,* 102(D14),

484   17051-17067

485

486   Kaufman, Y. J., Tanré D., & Boucher O. (2002). A satellite view of aerosols in the

487   climate system. *Nature,* 419, 215-223.

488

489   King M. D., Kaufman Y. J., Menzel W. P., & Tanré D .(1992). Remote sensing of Cloud,

490   Aerosol, and Water vapour properties from the Moderate Resolution Imaging

491   Spectroradiometer (MODIS). IEEE *Transactions on Geoscience and Remote Sensing,* 30

492   (1), 2-26

493

494   King M. D., Menzel W. P., Kaufman Y. J., Tanré D., Gao B., Platnick S., Ackerman S.

495   A., Remer L. A., Pincus R., & Hubanks P. A. (2003). Cloud and Aerosol Properties,

496   Precipitable Water, and Profiles of Temperature and Water Vapor from MODIS. IEEE

497   *Transactions on Geoscience and Remote Sensing,* 41, 442-458.

498

499   Levy R. C., Remer L. A., Marines J. V., & Kaufman Y., J. (2005). Evaluation of the

500   MODIS Aerosol Retrievals over Ocean and Land during CLAMS. *Journal of*

501   *Atmospheric Science,* 62, 974-992.

502

503   Levy R. C., Remer L. A., Mattoo S., Vermote E., F., & Kaufman Y. J. (2007a). Second-

504   generation operational algorithm: Retrieval of aerosol properties over land from inversion

505   of Moderate Resolution Imaging Spectroradiometer spectral reflectance. *Journal of*

506   *Geophysical Research,* 112, D13211, doi:10.1029/2006JD007811

507

508   Levy R. C., Remer L. A., & Dubovik O. (2007b). Global aerosol optical properties and

509   application to Moderate Resolution Imaging Spectroradiometer aerosol retrieval over

510   land. *Journal of Geophysical Research,* 112, D13210, doi:10.1029/2006JD007815

511

512   Lyamani H., Olmo F. J., Alcantara & Alados-Arboledas L. (2006). Atmospheric aerosols

513   during 2003 heat wave in southwestern Spain: Microphysicsl Columnar properties and

514   radiative   forcing.   *Atmospheric*   *Environment,*   40.   6465-6476,

515   doi:10.1016/j.atmosenv.2006.04.048.

516

517

518 Misra A., Jayraman A., & Ganguly D. (2008). Validation of MODIS derived aerosol

519 optical depth over Western India. *Journal of Geophysical Research*, 113, D04203, doi

520 10.1029/2007JD009075.

521

522 Morys M., F. M. Mims III., Hagerup S., Anderson S. E., Baker A., Kia J., & Walkup T.

523 (2001). design, calibration and performance of MICROTOPS II hand held ozone monitor

524 and sun photometer. *Journal of Geophysical Research*, 106, D13, doi:

525 10.1029/2001JD900103

526

527 Pandithurai G., Pinkaer R. T., Devara P. C. S., Takamura T., & Dani K. K. (2007).

528 Seasonal asymmetry in diurnal variation of aerosol optical characteristics over Pune,

529 western India. *Journal of Geophysical Research*, 112, D08208, doi

530 10.1029/2006JD007803.

531

532 Prasad A. K., Sing R. P., & Sing A. (2004). Variability of Aerosol Optical Depth Over

533 Indian Subcontient Using MODIS Data. *Journal of Indian Society of Remote Sensing*, 32

534 (4)

535

536 Prasad A. K., & Singh R. P. (2007). Comparison of MISR-MODIS aerosol optical depth

537 over INDO-Gangatic basin during the winter and pre-monsoon seasons (2000-2005).

538 *Remote Sensing of Environment*, 107, 109-119.

539

540

541   Remer L. A., &   Kaufman Y. J. (1998). Dynamic aerosol model: Urban/industrial

542   aerosol. *Journal of Geophysical Research*, 103 (D 12), 13,859-13,871.

543

544   Remer L. A., Kaufman Y. J., Tanré D., Mattoo S., Chu D. A., Martines J. V., Li R. R.,

545   Ichoku C., Levy R. C., Kleidman R. G., Eck T. F., Vermote E., & Holben B., N. (2005).

546   The MODIS Aerosol Algorithm, products, and validation. *Journal of   Atmospheric*

547   *Science*, 62, 947-973.

548

549   Retalis A., Hadjimitsis D. G., Michaelides S., Chrysoulakis N., Clayton C. R. I., &

550   Themistocleous K. (2010). Comparison of aerosol optical thickness with in situ visibility

551   data over Cyprus. *Natural Hazards and Earth System Science*, 10, 421-428.

552

553   Schaap M., Timmermans R. M. A., Koelemeijer R. B. A., Leeuw G. De., & Builtjes P. J.

554   H. (2008). Evaluation of MODIS aerosol optical thickness over Europe using sun

555   photometer observations. *Atmospheric Environment* 42, 2187-2197.

556

557   Singh R. P., Day S., Tripathi S. N., & Tare V. (2004). Variability of aerosol parameters

558   over Kanpur, northern India. *Journal of Geophysical Research*, 19 (D23206), doi:

559   10.1029/2004JD004966

560

561   Smirnov A., Holben B. N., Dubovik O., O' Nill N. T., Eck T. F., Westphal D. L., Goroch

562   A. K., Pietras C., & Slutsker I. (2002). Atmospheric Aerosol Optical Properties in the

563   Persian Gulf. *Journal of Atmospheric Science*, 59, 620-634.

564

565   Sumit K., Devara P.C.S., Dani K.K., Sonbawne S.M., & Saha S.K. (2011). Sun-sky

566   radiometer–derived column-integrated aerosol optical and physical properties over a

567   tropical urban station during 2004–2009. *Journal of Geophysical Research*, 116

568   (D10201), doi:10.1029/2010JD014944.

569

570   Tanré D., Kaufman Y. J., Herman M., & Mattoo S. (1997). Remote sensing of aerosol

571   properties over oceans using the MODIS/EOS spectral radiance. *Journal of Geophysical*

572   *Research*, 102(D14), 16971-16988.

573

574   Tripathi S. N., Day S., Chandel A., Srivastava S., Sing R. P., & Holben B. N. (2005).

575   Comparision of MODIS and AERONET derived aerosol optical depth over Ganga Basin,

576   India. *annals Geophysicae*, 23, 1093-1101.

577

578   Venkataraman C., Habib G., Fernande A., Miguel A. H., & Friedlander S. K. (2005).

579   Residential Biofuels in South Asia: Carbonaceous Aerosol Emissions and Climate

580   Impacts. *Science*, 307 (5714), 1454-1456.

581

582   Verneker K. G., Mohan B., Saxena S., & Patil M. N. (1993). Characteristics of the

583   atmospheric boundary layer over a tropical station as evidenced by tethered balloon

584   observations. *Journal of Applied Meteorology*, 32, 1426-1432.

585

586

587   Xia X., Wang P., Chen H., Philippe G. & Zhang W. (2005). Ground based remote

588   sensing of aerosol optical properties over north China in Spring. *Journal of Remote*

589   *Sensing*, 9 (4), 429-437.

590

591   Zhao T. X. –P., Stowe L. L., Smirnov A., Crosby S., Sapper J., & McClain C. (2002).

592   Development of a Global Validation Package for Satellite Oceanic Aerosol Optical

593   Thickness Retrieval Based on AERONET Observations and Its Application to

594   NOAA/NESDIS Operational Aerosol Retrievals. *Journal of Atmospheric Science*, 59,

595   294-312

Table I: Observed seasonal columnar volume size distribution parameters of aerosol particles and Angstrom Exponent (α)

Season	V_a	R_a	σ_a	V_c	R_c	σ_c	α
Winter	0.047	0.148	0.025	0.053	3.857	0.028	1.307 (±0.189)
Premonsoon	0.044	0.113	0.027	0.087	3.857	0.047	0.851 (±0.315)

V is columnar volume of atmospheric aerosol particles per unit cross section of the atmospheric column, R is the radius and σ is standard deviation (subscripts "a" and "c" stands for accumulation mode and coarse mode respectively) and α is mean Angstrom Exponent.

Table II: Results of regression analysis for MODIS (Terra and Aqua) derived AOD against AERONET measurements at 550 nm during 2008-09 and 2009-10

Year		Slope	Intercept	R	RMSE	% in EE	N
2008-09	Terra	0.86	0.05	0.80	0.09	83.89	118
	Aqua	1.05	-0.01	0.78	0.10	73.26	101
2009-10	Terra	0.65	0.11	0.70	0.11	68.07	119
	Aqua	0.73	0.11	0.73	0.11	69.79	96
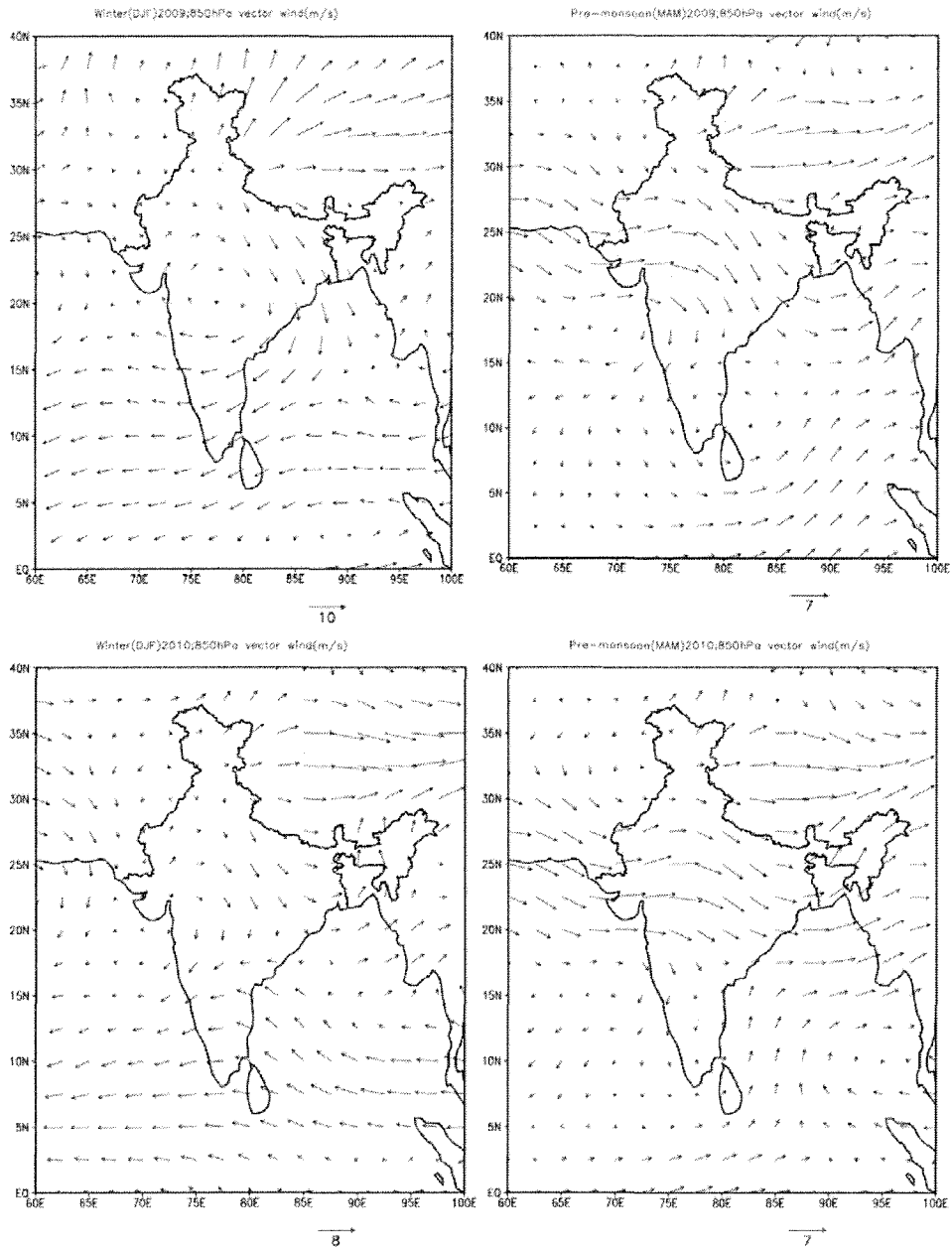
Figure 1:- NCEP /NCAR reanalysis mean vector wind composites at 850 hPa level for winter and pre-monsoon season during 2008-09 and 2009-10
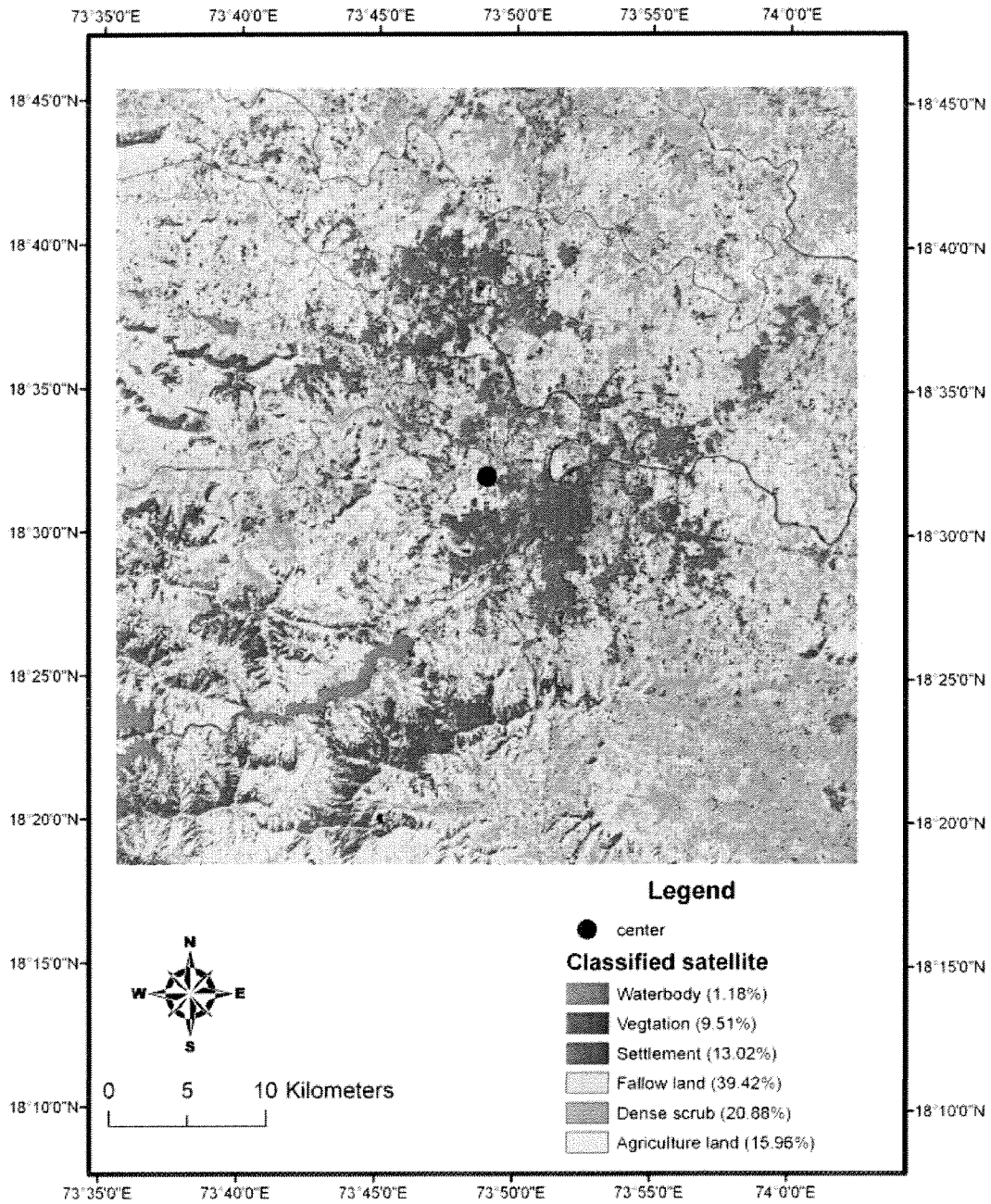
Figure 2: Land cover and land use of the study region (50 x 50 grid box)
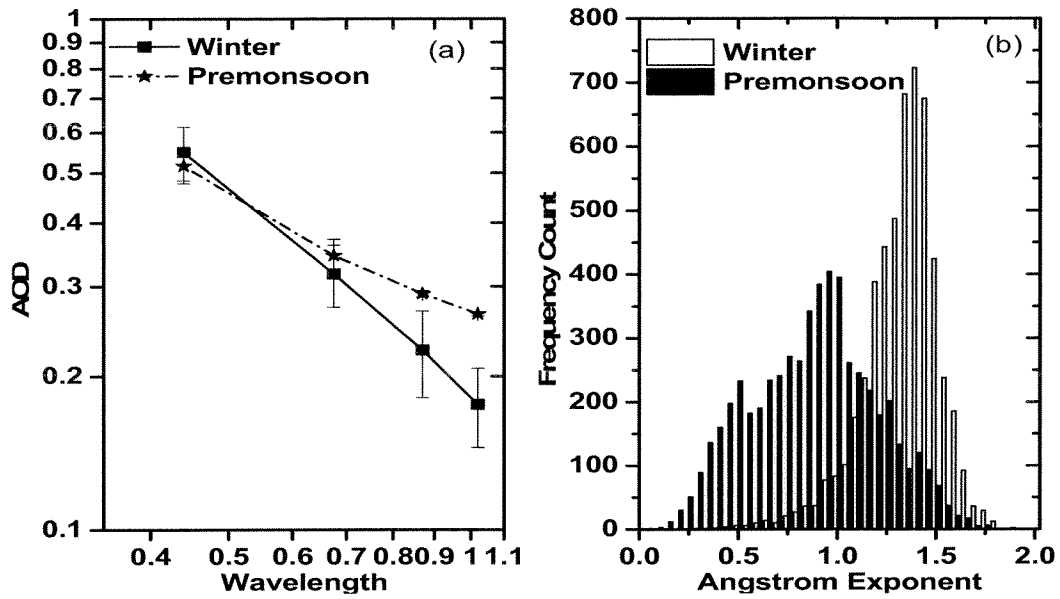
Figure 3: (a) Spectral variation of AOD and (b) frequency distribution of Angstrom exponent over Pune using AERONET measurements for the period Dec 2008 – May 2010.
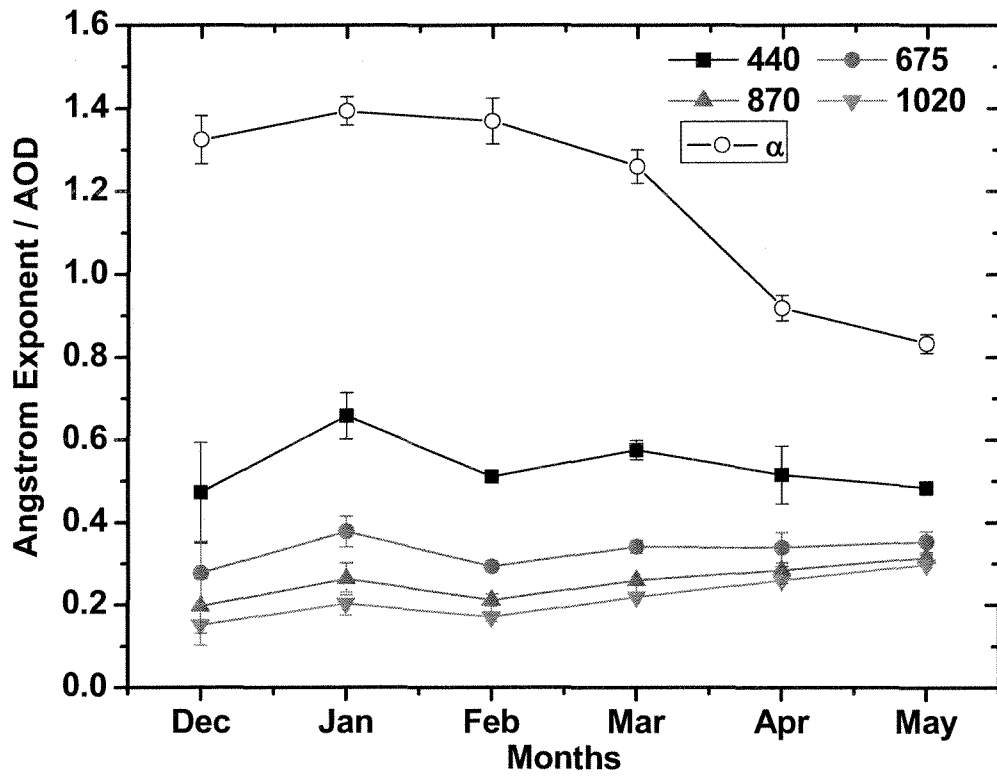
Figure 4: Monthly mean value of aerosol optical depth and Angstrom exponent (α) using AERONET data during Dec 2008-May 2010.
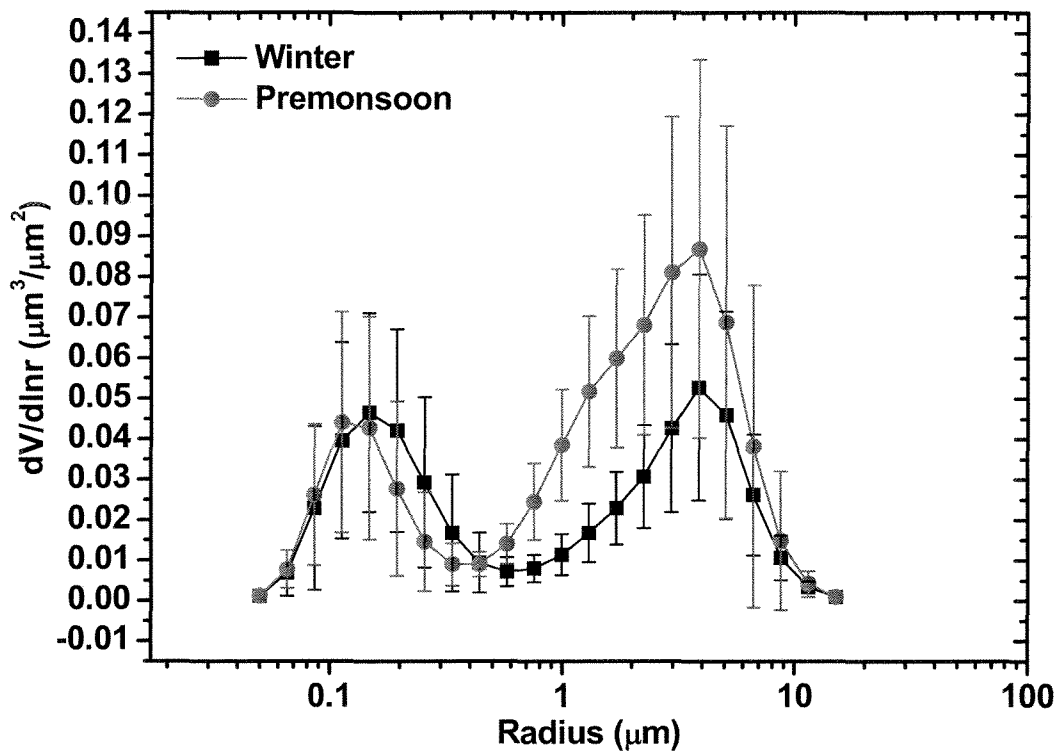
Figure 5: Seasonal variation of aerosol columnar volume size distribution over Pune using AERONET measurements during the period Dec 2008 – May 2010.
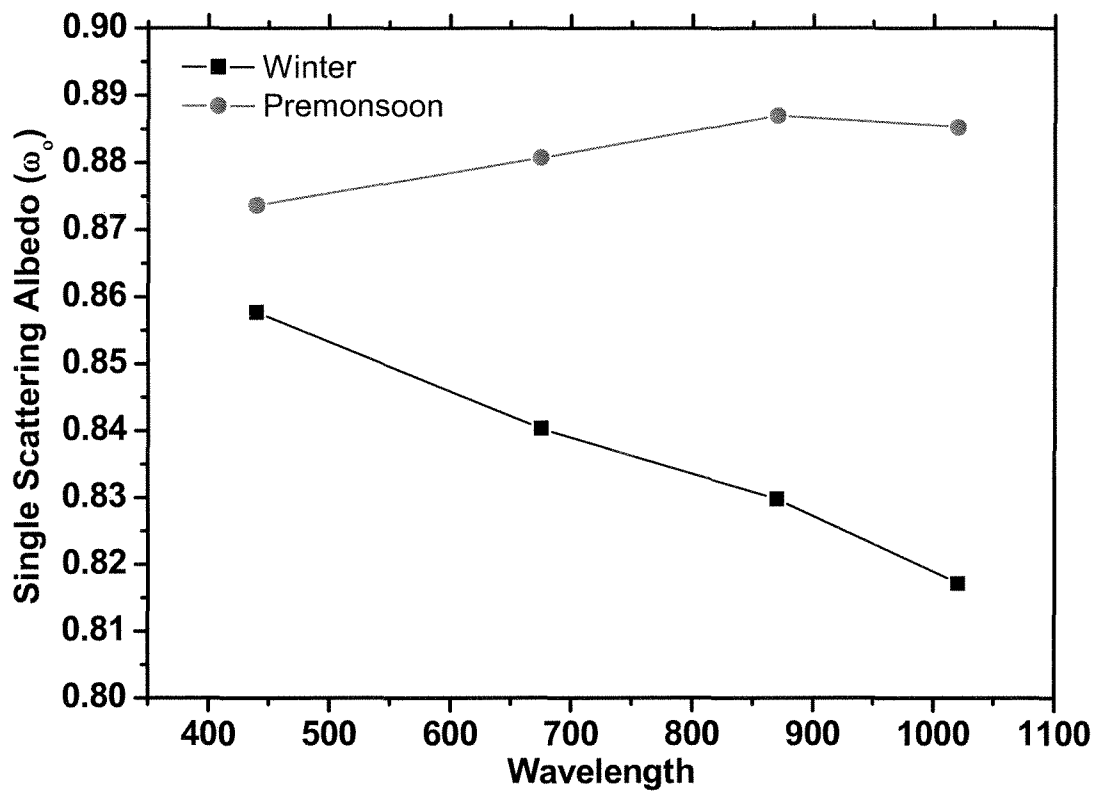
Figure 6: Wavelength dependency of single scattering albedo over Pune using AERONET
measurements for the period Dec 2008 – May 2010.
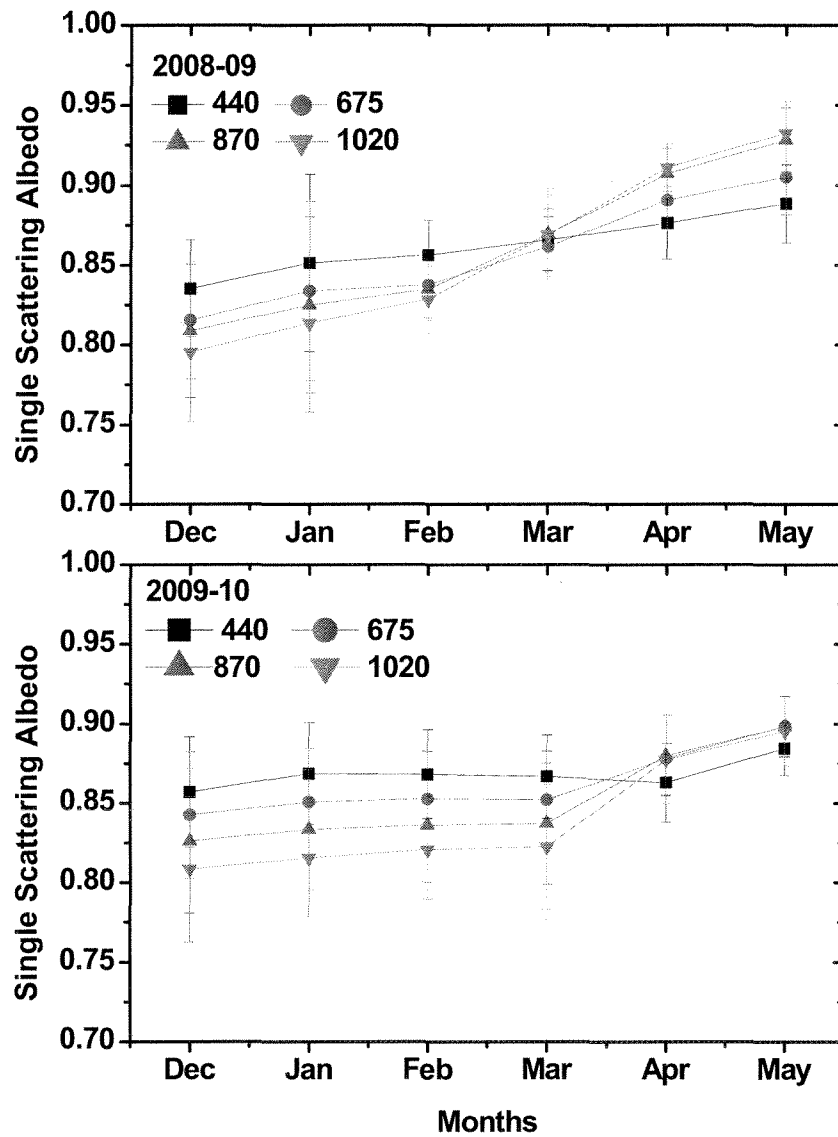
Figure 7: Monthly variation of single scattering albedo over Pune using AERONET measurements during 2008-09 and 2009-10.
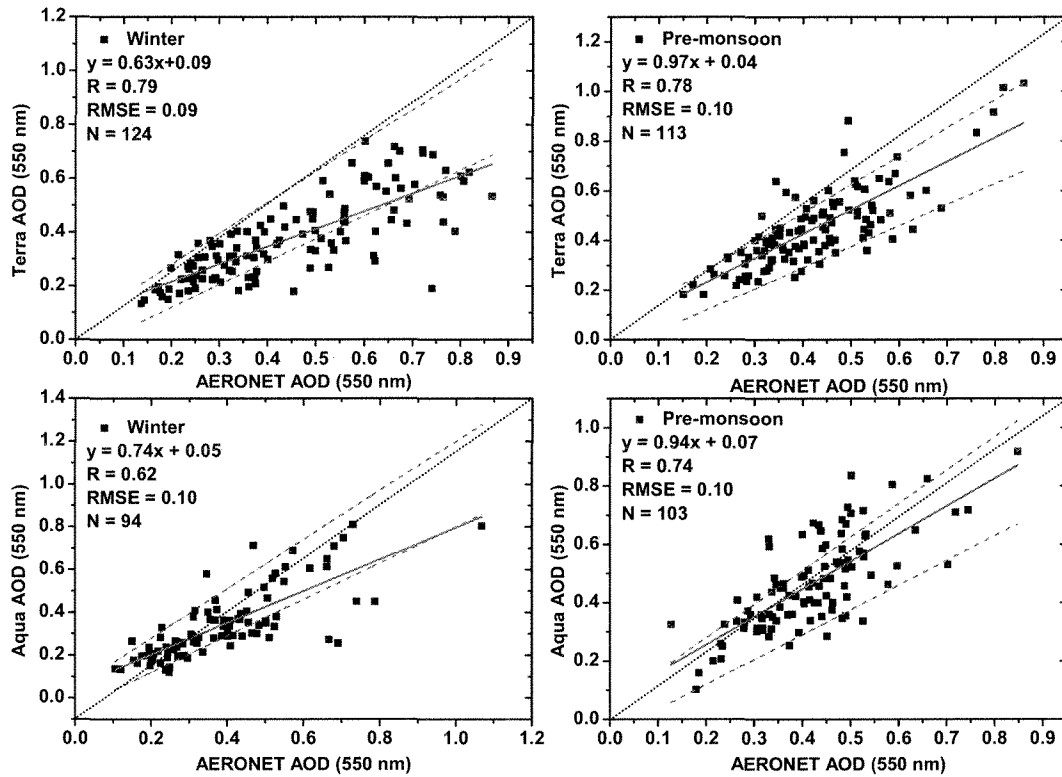
Figure 8: Scatter plots of MODIS (Terra and Aqua) AOD retrievals against AERONET derived AODs, during the winter and pre-monsoon during 2008-2010. (The thick solid lines, dashed lines and dotted lines represent linear regression, EE and 1:1 line respectively).
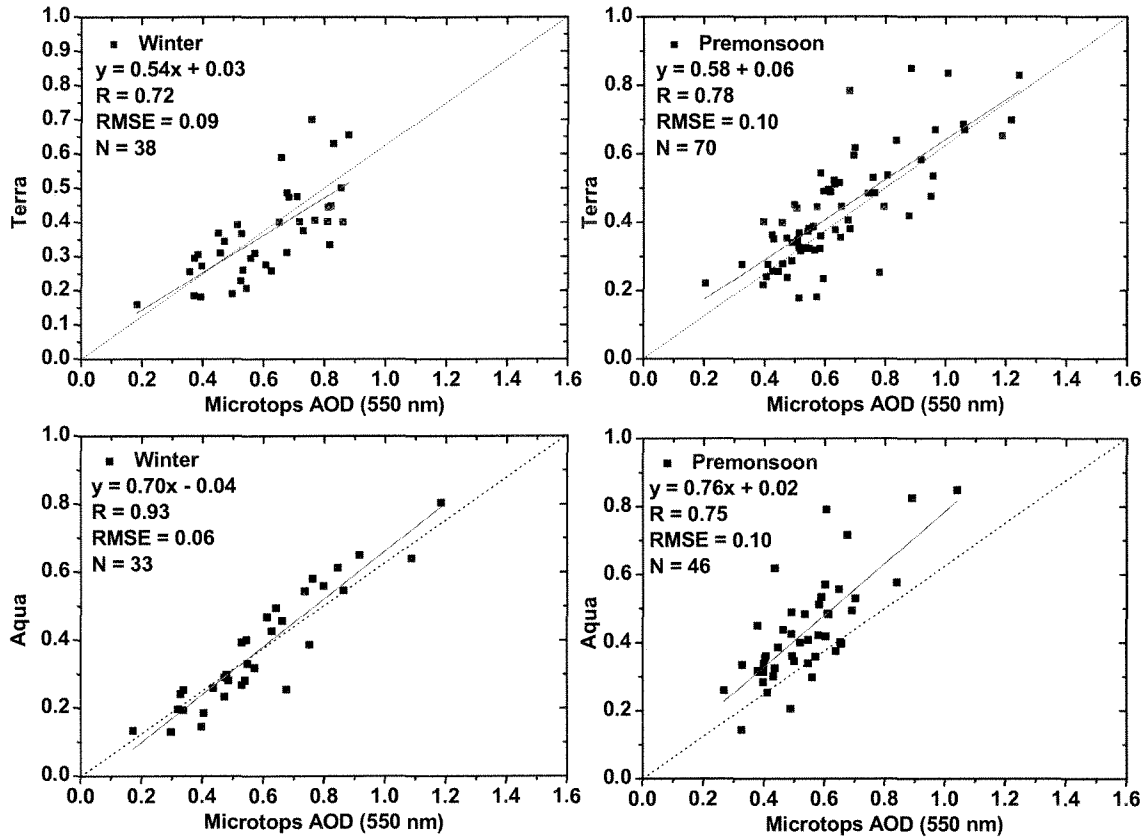
Figure 9: Scatter plots of MODIS (Terra and Aqua) AOD retrievals against Microtops measured AODs, during the winter and pre-monsoon during 2008-2010. (The solid lines represent linear regression and dotted lines are 1:1 lines).
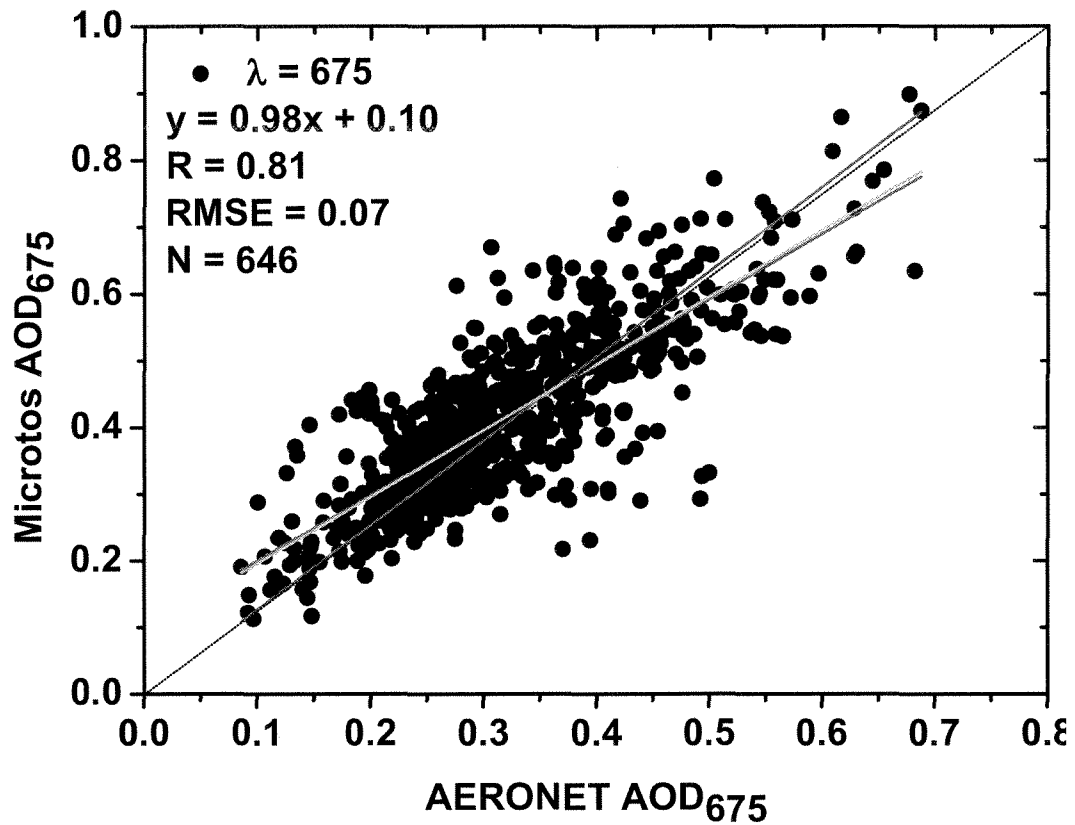
Figure10: Scatter plot of AERONET and Microtops AOD measurements at 675 nm during 2008-2010. (Red line is regression line and blue and green lines are forced lines at intercept = 0 and slope = 1 respectively; dotted black line is 1:1 line).
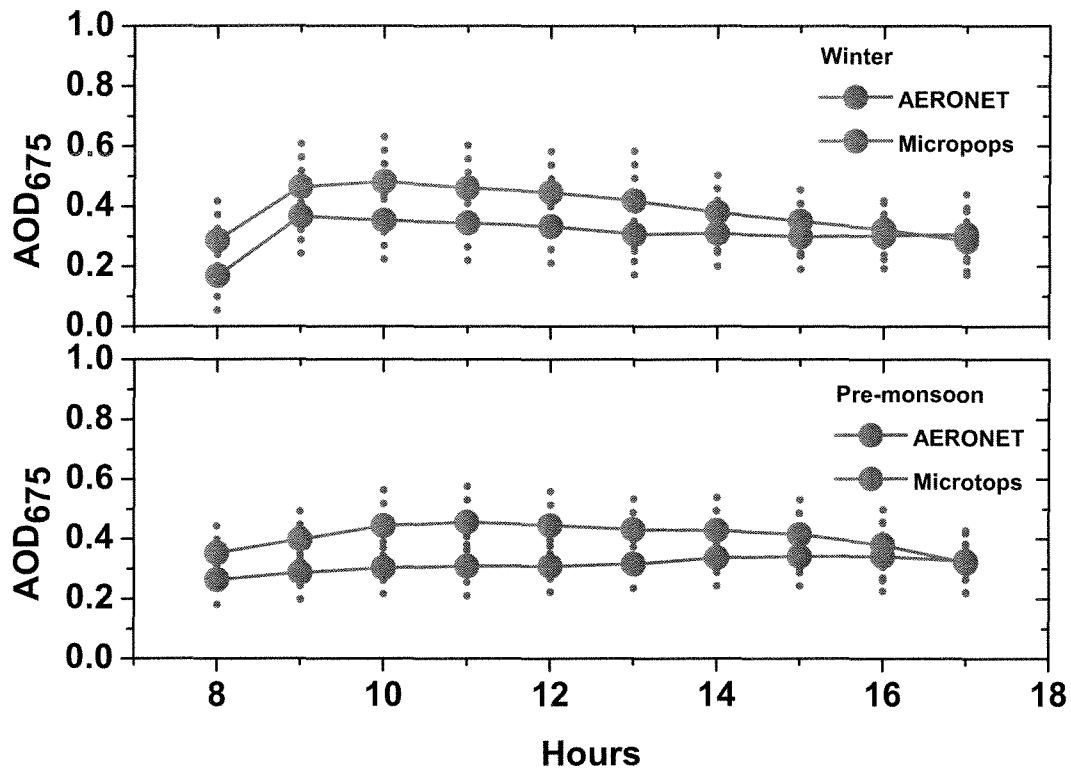
Figure 11: Seasonal inter-comparison of AERONET and Microtops II Sun-photometer
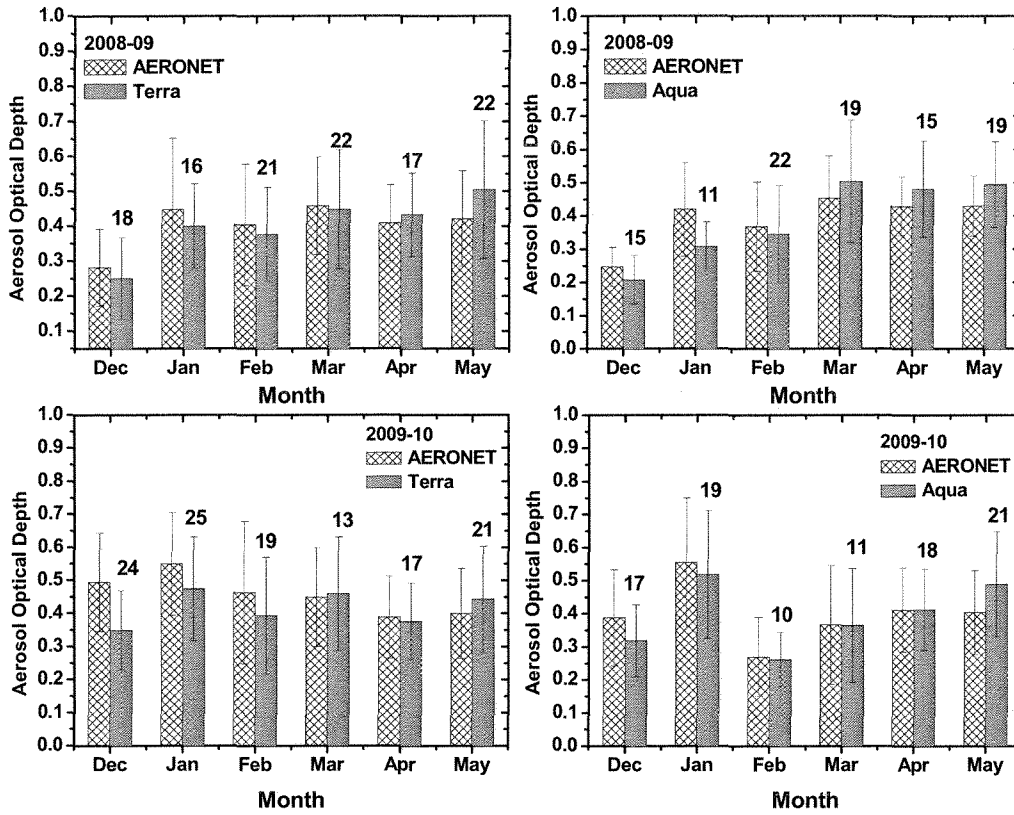during 2008-2010

Figure 12: Monthly mean AODs for MODIS (Terra and Aqua) and AERONET during 2008-2009 and 2009-2010 over Pune.
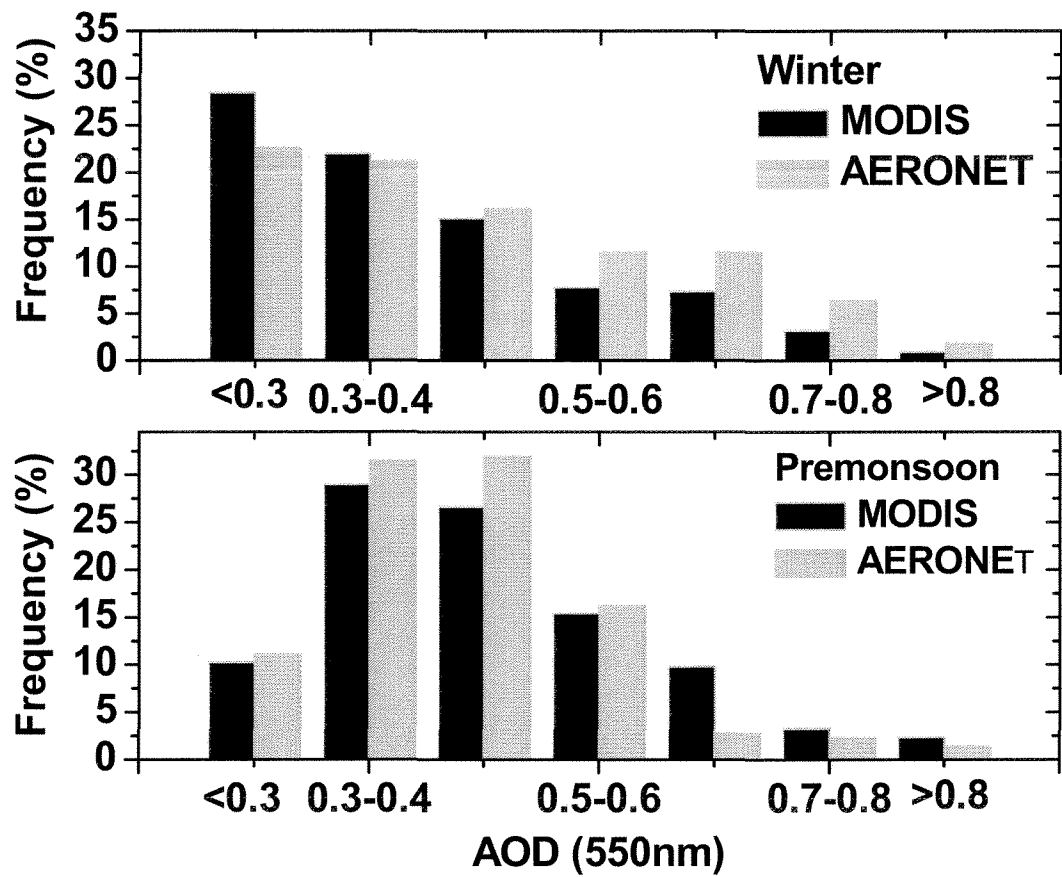
Figure 13: Seasonal frequency distribution of MODIS and AERONET AODs during Dec 2008-May 2010.